PROGRESS REPORT (Nov. 96):
Tables and figures final; text will be completely revised

Noise Sensitivity of BRDF and Albedo Retrieval From the Earth Observing System MODIS and MISR Sensors With Respect to Angular Sampling

Philip Lewis[1] and Wolfgang Wanner[2]

[1] *Remote Sensing Unit, Dept. of Geography, University College London, London, UK*
[2] *Center for Remote Sensing and Dept. of Geography, Boston University, Boston, MA*

Abstract

The sensitivity of the Ambrals semiempirical BRDF model to random noise in observed multiangular reflectances is investigated. The mathematical properties of kernel-driven BRDF models allow to derive analytically so-called weights of determinations or noise inflation factors that quantify the expected noise found in retrieved parameters like nadir-view reflectance or albedo at various solar zenith angles, or in the BRDF model parameters. The study is carried out using simulated angular sampling as is to be expected from the MODIS and MISR instruments to be flown on the EOS-AM platforms as a function of latitude, day of year and sampling period. A similar study is carried out for comparison using the modified RPV BRDF model. Results show that for both models the retrieved parameters reflectance and albedo the noise amplification factors are less than one (less noise present than was in the original data, i.e., the retrievals are stable with respect to random noise). The BRDF model parameters themselves, especially for the modified RPV model, are found to be more susceptible to noise. Differences in noise sensitivity between different model variants and sampling scenarios are further explored. This study is relevant with respect to the reliability to be expected from the planned operational BRDF/albedo products from the MODIS and MISR instruments.

1. Introduction

Global space-based retrievals of the bidirectional reflectance distribution function (BRDF) and albedo over land will be possible in the near future using the Earth Observing System's (EOS) MODIS and MISR sensors or the POLDER instrument. BRDF information is useful for normalizing satellite-acquired data sets and for deriving key surface parameters, mainly atmospherically corrected albedo for use in climate studies.

Little work, however, has been done on the sensitivity of BRDF and albedo retrievals to angular sampling patterns even though the impact of these on product accuracy is possibly substantial. With any instrument, the angular distribution of samples obtainable in a given time period will vary with geographic latitude and time of year, and be also determined by instrument and orbit characteristics. Cloud masking will further reduce the set of available angular reflectances. In this paper we evaluate in a practical case the impact of angular sampling effects on BRDF and albedo derivation.

Two effects mainly have an influence on retrieval accuracy as a function of angular sampling:
(1) Sensitivity to random noise. Analysis is carried out under the assumption that the RMSE found in

inverting a model against observations is due to random "noise-like" errors in the observed reflectances, due for example to fluctuations in surface properties, misregistration, atmospheric correction errors etc.
(2) Misfit sensitivity. Analysis is carried out under the assumption that the RMSE found in inversion is due to an inherent partial inability of the model used to fit the observations even in the absence of "noise", and to infer completely from limited angular sampling the BRDF shape observed. Investigating this effect is important in view of the many assumptions that are commonly made in operationally feasible BRDF models.

In this paper, we focus on the noise sensitivity analysis alone, although the misfit analysis is of equal importance. We study the behavior of the semiempirical Ambrals BRDF model (Wanner et al., 1995, 1997) under conditions of sampling by MODIS and MISR, and how the semiempirical Rahman model (Rahman et al., 1993) behaves under the same circumstances.

2. The Experiment

We here investigate sampling effects with respect to the MODIS BRDF/albedo product (Strahler et al., 1996; Wanner et al., 1997), using the sampling patterns and BRDF models characterizing it. The product is slated for production at a spatial resolution of one kilometer once every 16 days and in seven spectral bands from combined MODIS-AM and MISR data starting in 1998. The MODIS-AM sensor is an across-track imager with a swath width of 2330km, and a repeat rate shorter than 2 days (mostly shorter than 1 day). MISR is an along-track imager with a swath width of 364km using four fore-, four aft- and one nadir-pointing camera. The two-look repeat rate is 16 days. In this time, each sensor produces a string of observations across the viewing hemisphere with rather constant relative azimuth and solar zenith angles. The two strings from the two instruments are nearly orthogonal; their respective azimuthal distance from the principal plane varies with latitude and time of year, as does the mean solar zenith of the observations and the number of observations from MODIS.

The analysis was carried out for the Ambrals BRDF model that will be used in the production of the MODIS BRDF/albedo product. The kernel combinations used in that model are: RossThick-LiSparse, RossThin-LiSparse, RossThin-LiDense, and RossThick-LiDense (Wanner et al., 1995). These are capable of modelling a wide variety of volume and surface scattering behavior and which will be employed depending on the scattering behavior observed.

Retrievals investigated are for nadir-view reflectance and directional-hemispherical ("black-sky") albedo. Both of these quantities are studied for retrievals at the mean sun angle of the observations ("interpolation") and for nadir sun zenith angle ("extrapolation", the amount of extrapolation depending on the sun angle of observations, which depends on the latitude and the time of year of the observations). Additionally, bihemispherical albedo ("white-sky albedo") is studied.

MODIS and MISR sampling was simulated using the Xsatview software (Barnsley et al., 1994). The viewing and illumination geometries were constructed for 9 latitudes between 80 degrees south and 80 degrees north, and for 8 different 16-day time periods throughout the year.

3. Noise Sensitivity of the Ambrals Model

3.1. Method

The behavior of kernel-driven linear models under the conditions of limited and varying angular sampling can be studied analytically due to the mathematical form of these models. It is given by the the so-called "weights of determination", calculated using theory that originates with Gauss (Whittaker and Robinson, 1960). Kernel-driven models give the reflectance R in form of a sum, $R = \sum f_i k_i$, where f_i are the model

parameters and k_i are mathematical functions ("kernels") giving basic BRDF shapes depending only on sampling geometry.

The theory of least squares and related statistical analyses permit the derivation of unbiased estimates of model parameters and linear combinations of model parameters (such as reflectances at given angles and albedos for kernel-driven models). The techniques also directly provide estimates of the variance in these quantities. An overview of the relevant tools for analysis is provided below, but it is worth first considering the nature of "error" in this context. The theory used here and that used in most model inversions in the field of BRDF modelling is based on the assumption that the model is suitable for modelling the reflectance at some given location on the globe. Thus, if a model is "fitted" (in the sense of providing unbiased estimates of the model parameters) to a set of sample observations, then the model should be capable of predicting the reflectances (or derived quantities such as albedo-related terms) at viewing and illumination angles other than those sampled. The theory assumes that any deviation from a perfect fit in an over-constrained case (number of samples larger than number of model parameters) is due to error in observation. Related statistical theory tends to assume further that the variation in reflectance at each observation angle is normally distributed and of equal variance over the reflectance function (if the variance of the reflectance varies in some predictable way over the observation angles, this can be taken into account by weighting the observations). The "error" in a model fit term which is minimized in "fitting" the model, the root mean squared error (RMSE), provides an estimate of this variance in observation. Such fluctuations may indeed arise, due, for example, to uncertainty in atmospheric correction, registration or resampling. Some of these fluctuations may cause normally distributed variation in the data, and others, such as poor specification of the atmospheric intrinsic path radiance, may cause bias. The former is well-treated in the approach followed in this paper, and the latter may be taken into account in describing the additional expected error if an estimate of the bias is produced.

The key to understanding the behavior of kernel-driven linear models in the presence of random noise in the observed data under the conditions of limited and varying angular sampling is the variation of the so-called "weights of determination" of the model parameters, derived reflectances and derived albedo measures found from model inversion. These weights allow an estimation of the expected error in the terms under consideration, which can be expressed as (Whittaker and Robinson, 1960)

$$\epsilon_u = e\sqrt{\frac{1}{w_u}}, \tag{1}$$

where e is the estimate of standard error in the observed data (approximated by the RMSE in model fitting), and $1/w_u$ is the weight of determination of term u under the sampling configuration considered. The weight of determination is formed through

$$\frac{1}{w_u} = [U]^T[M^{-1}][U], \tag{2}$$

where U is a vector composed of the weighting of the kernels in some linear combination of the kernels which results in the term u under consideration, and M^{-1} is the inverse matrix providing the solution of the least-squares inversion problem for the linear model.

For example, to obtain the weight of determination of the parameter $f_0 = f_{iso}$ of a kernel-driven model, $[U]^T = (1,0,0)$. The weight of determination of directional-hemispherical reflectance at solar zenith angle θ_s is formed from $[U]^T = (1, \overline{k_1(\theta_s)}, \overline{k_2(\theta_s)})$, where $\overline{k_i}$ are the respective directional-hemispherical integrals of the kernels used. The weight of determination of bihemispherical reflectanc is formed from $[U]^T = (1, \overline{\overline{k_1}}, \overline{\overline{k_2}})$, where two bars tand for the respective bihemispherical integral. The weight of determination of the reflectance at some combination of viewing and illumination angles, $(\theta_v, \theta_s, \phi)$, is given by forming $[U]^T = (1, k_1(\theta_v, \theta_s, \phi), k_2(\theta_v, \theta_s, \phi))$.

The weight of determination depends on the sampling scheme under consideration because M^{-1} depends on it. The weight of determination also depends on the number of samples, N, and contains the factor $1/\sqrt{N}$.

Increasing N decreases the expected error because the errors are assumed to be randomly distributed at each observation angle. Thus, we can already begin to understand that factors such as cloud cover, which will reduce N from the maximum ideal number considered in this study to N', will tend to increase the expected error even if the angular distribution of samples remains roughly the same. The increase in each term under consideration is given by $\sqrt{N/N'}$.

Note that this analysis is independent of any specific BRDF function.

3.2. Results for the Ambrals Model

In an extensive investigation, we have studied the sensitivity to random noise of the several Ambrals BRDF model variants listed above using sampling for a variety of combinations of the MODIS and MISR sensors, and for different periods of data accumulation. Table 1 lists the weights of determination found for albedo and nadir view reflectance retrieval in interpolation and extrapolation for the different Ambrals model kernel combinations. Nearly all numbers are smaller than 1, indicating stability with respect to noise amplification in deriving the respective quality.

Table 2 investigates median error ranges (the ranges reflecting variations with kernel combination used; the median being with respect to latitude and day of year) for different sampling scenarios using MODIS and MISR on the EOS-AM-1 platform and MODIS on the PM platform. The MISR BRDF/albedo product, which will be produced using the BRDF model by Rahman et al. (1993), will be based on a 9-day sampling period, whereas the MODIS BRDF/albedo product will be built from data acquired during 16-day periods. Since the RossThick and LiDense kernels are least independent in their angular characteristics, the RossThick-LiDense kernel combination is most susceptible to noise of all combinations. Therefore, we list results separately for using this combination and for using those kernels separately along with the other kernel combinations. The lower part of the table lists relative changes in accuracy of the different sampling schemes as measured against the combined MODIS and MISR 16-day sampling.

Table 2 shows that albedo and nadir-view reflectance may be stably retrieved both in interpolation and extrapolation of the solar zenith angle. This is also true for 9-day MISR sampling, showing that MISR angular sampling is very suitable for these retrievals. Using MODIS alone introduces susceptibility to noise that is not desired. The MODIS-PM instrument is a partial, but not a full substitute for the MISR instrument, the advantage of MODIS-PM being, however, that it will feature the same 7 land-designated spectral bands as the MODIS-AM instrument, whereas MISR has only 4 bands.

Table 3 lists the worst-case ranges of the noise sensitivities found. "Worst-case" refers to the most unfavorable choice of kernel combination; the numbers given are the range numbers that include two thirds of the data for all latitudes and times of year.

Figure 1 shows the weights of determination found for the different retrievals when using the RossThick-LiSparse model, chosen as a typical example. Curves represent different days in the first half of the year. Panel (f) shows the error expected when extrapolating black-sky albedo in sun zenith angle for different latitudes and sampling in the first 16-day period of the year. One can see that extrapolation towards nadir is less problematic than extrapolation to large zenith angles for all latitudes, the beginning of the rise being determined by the sun zenith angle at which the observations were made.

Overall, the noise sensitivity of the Ambrals BRDF model with respect to BRDF and albedo retrieval at the sun zenith angles investigated is such that in the absence of clouds noise-like effects in the observations lead to a usually much smaller error in the derived quantities than was present in the reflectances. Under conditions where observations will be lost to clouds, the sensitivity will increase, but the noise inflation factor will still be mostly smaller than unity.

Figure 2 shows the noise sensitivity of the model parameters themselves (note that the isotropic parameter is identical with nadir-view, nadir-sun reflectance, shown in Figure 1). They are more susceptible to noise than the derived quantities due to possible tradeoffs between parameter values that do not affect, for example,

the value of albedo. This means that while albedo and reflectance retrievals are robust, interpretation of the model parameters themselves, desired with respect to correlating them with land cover types, is more problematic. See also the numbers in Tables 1, 2 and 3.

4. Noise Sensitivity of the modified RPV model

The noise sensitivity of the RPV BRDF model by Rahman et al. (1993) as modified by Martonchik (Engelsen et al., 1996) was also investigated for comparison and in order to reveal whether the properties found are related to the Ambrals model in particular or whether they might pertain to 3-parameter models in general.

The modified RPV model is not fully linear, making the analytical investigation of noise sensitivity along the lines of the Ambrals BRDF model impossible. However, an equivalent weight of determination may be constructed from the RMSE and the variation found in the derived quantity, albedo or reflectance. This was done by computing 250 realizations of noisy data for each of 5 magnitudes of noise up to 5 percent absolute of the reflectance (keeping the resulting reflectance is non-negative).

Due to the nonlinear nature of the modified RPV model, the analysis will also depend on land cover type and wave band. The analysis was carried out for the red and the near-infrared using four different data sets measured by Kimes (1983) and Kimes et al. (1985, 1986), namely BRDF observations of corn, a plowed field, a hardwood forest and a grass lawn. These represent four types of BRDFs, a broadleaf crop, a barren scene, a forested scene, and a grass-like land cover.

Table 4 gives ranges of the inferred equivalent weights of determination. Numbers are similar to those found for the Ambrals BRDF model, showing that both models do a good job in the stability of the retrievals with respect to random noise.

Figure 3 shows red and near-infrared weights of determinations as a function of latitude for a 16-day period beginning the first day of the year for the four land cover types used (solid and dotted lines). Also given is the result for the RossThick-LiSparse Ambrals model kernel combination (dashed line), showing that where one model has increased sensitivity to noise the other one does, too.

Figure 2 shows the sensitivity of the three modified RPV model parameters. The second and third parameters, the two describing BRDF shape, are extremely susceptible to noise. This does not translate to noisy retrievals of reflectance and albedo, but will make very difficult using and interpreting them directly. The cause of this sensitivity is probably internal redundancy in the way these parameters affect overall BRDF shape, perhaps caused by the hotspot term the model contains that allows tradeoffs between parameters under limited angular sampling. However, since the model retrieves albedo and reflectance very well, this does not constitute a major problem in terms of physical quantities to be retrieved.

A more detailed investigation is under way.

5. Conclusions

Retrievals of BRDF and albedo using the Ambrals BRDF model is stable against random noise-like variations in the reflectances used that may be due for example to fluctuations in surface properties, misregistration, atmospheric correction errors etc. This holds both for retrieval of BRDF and albedo at the mean sun angle of observation and for extrapolation of the retrieval to a nadir sun zenith angle. Where the Ambrals BRDF model shows increased susceptibility to noise, the modified RPV model does, as well, indicating that the source of the problem lies in the geometric distribution of angular samples available, not with the model. Generally, the modified RPV model is as capable of retrieving BRDF and albedo from MODIS and MISR sampling as the Ambrals BRDF model. The respective model parameters themselves are more noisy than the derived quantities BRDF and albedo for both models, but much more so for two of the three parameters of the modified RPV model. In terms of using different instruments for sampling, a combination

of MODIS and MISR leads to excellent retrievals in terms of noise sensitivity. Using MISR only is also feasible. Using MODIS alone may represent a problem due to the less favorable angular sampling properties of this instrument.

Acknowledgments
We thank Mike Barnsley and Kevin Morris for providing the Xsatview software for orbital modeling, without which this work would have been impossible. This work was partly supported by NASA under NAS5-31369.

References

Barnsley, M. J., A. H. Strahler, K. P. Morris, and J.-P. Muller, Sampling the surface bidirectional reflectance distribution function (BRDF): Evaluation of current and future satellite sensors, *Remote Sens. Rev. 8*, 271–311, 1994.

Engelsen, O., B. Pinty, M. M. Verstraete, and J. V. Martonchik, Parametric bidirectional reflectance factor models: evaluation, improvements and applications, *Report, Joint Research Centre of the European Commission, EU 16426,*, 114 pp., 1996.

Kimes, D. S., Dynamics of directional reflectance factor distribution for vegetation canopies, *Appl. Opt., 22(9)*, 1364–1372, 1983.

Kimes, D. S., W. W. Newcomb, C. J. Tucker, I. S. Zonneveldt, W. van Wijngaarden, J. de Leeuw, and G. F. Epema, Directional reflectance factor distributions for cover types of Northern Africa, *Remote Sens. Env., 18*, 1–19, 1985.

Kimes, D. S., W. W. Newcomb, R. F. Nelson, and J. B. Schutt, Directional reflectance distributions of a hardwood and a pine forest canopy, *IEEE Trans. Geosci. Remote Sens., 24*, 281–293, 1986.

Rahman, H., B. Pinty, and M. M. Verstraete, Coupled surface-atmosphere reflectance (CSAR) model, 2, Semiempirical surface model usable with NOAA advanced very high resolution radiometer data, *J. Geophys. Res., 98*, 20,791–20,801, 1993.

Strahler, W. Wanner, A. H., C. B. Schaaf, J.-P. Muller, M. J. Barnsley, R. d'Entremont, B. Hu, P. Lewis, X. Li, and E. V. Ruiz de Lope, MODIS BRDF/albedo product: Algorithm theoretical basis document, *NASA EOS-MODIS Doc.*, version 4.0, 1996.

Wanner, W., X. Li, and A. H. Strahler, On the derivation of kernels for kernel-driven models of bidirectional reflectance, *J. Geophys. Res., 100*, 21077–21090, 1995.

Wanner, W., A. H. Strahler, B. Hu, X. Li, C. L. Barker Schaaf, P. Lewis, J.-P. Muller, and M. J. Barnsley, Global retrieval of bidirectional reflectance and albedo over land from EOS MODIS and MISR data: theory and algorithm, *J. Geophys. Res.*, in press, 1997.

Whittaker, E., and G. Robinson, *The Calculus of Observations*, Blachie and Son, Glasgow, 397 pp., 1960.

Table 1: WEIGHTS OF DETERMINATION FOR MODIS-AM/MISR 16-DAY SAMPLING: TYPICAL SMALL, MEDIAN AND LARGE ERROR FOR DIFFERENT KERNEL-DRIVEN BRDF MODELS

MODIS–AM+MISR 16-Day Sampling	kernel 1	kernel 2	low	median	high	low	median	high
			Nadir-View Reflectance			Black-Sky Albedo		
Interpolation	RossThin		0.17	0.21	0.24	0.14	0.17	0.19
$\theta_s = \langle\theta_s\rangle$	RossThick		0.17	0.18	0.21	0.12	0.16	0.17
	LiSparse		0.14	0.19	0.25	0.13	0.17	0.18
	LiDense		0.15	0.18	0.19	0.12	0.16	0.18
	RossThin	LiSparse	0.18	0.23	0.27	0.14	0.17	0.19
	RossThin	LiDense	0.17	0.22	0.24	0.15	0.18	0.20
	RossThick	LiSparse	0.18	0.23	0.28	0.13	0.17	0.18
	RossThick	LiDense	0.17	0.19	0.22	0.13	0.16	0.18
Extrapolation	RossThin		0.19	0.23	0.25	0.15	0.17	0.19
$\theta_s = 0$	RossThick		0.16	0.17	0.19	0.16	0.18	0.21
	LiSparse		0.38	0.44	0.53	0.16	0.18	0.28
	LiDense		0.48	0.62	0.71	0.18	0.21	0.28
	RossThin	LiSparse	0.38	0.45	0.55	0.16	0.18	0.33
	RossThin	LiDense	0.73	0.93	1.08	0.19	0.28	0.49
	RossThick	LiSparse	0.40	0.46	0.55	0.17	0.21	0.36
	RossThick	LiDense	1.03	1.35	1.71	0.39	0.52	0.63
						White-Sky Albedo		
Global, $\int \theta_s d\theta_s$	RossThin					0.14	0.31	0.64
	RossThick					0.14	0.18	0.34
	LiSparse					0.18	0.30	0.43
	LiDense					0.13	0.17	0.23
	RossThin	LiSparse				0.19	0.36	0.64
	RossThin	LiDense				0.21	0.42	0.82
	RossThick	LiSparse				0.19	0.34	0.58
	RossThick	LiDense				0.16	0.36	1.05
			Parameter f_{vol}			Parameter f_{geo}		
Parameters	RossThin		0.04	0.14	0.25			
	RossThick		0.32	0.89	1.74			
	LiSparse					0.18	0.27	0.31
	LiDense					0.34	0.46	0.57
	RossThin	LiSparse	0.05	0.15	0.30	0.19	0.28	0.36
	RossThin	LiDense	0.07	0.17	0.29	0.45	0.60	0.69
	RossThick	LiSparse	0.33	0.89	1.76	0.20	0.27	0.31
	RossThick	LiDense	0.62	1.86	4.14	0.60	0.86	1.34

Table 2: MEDIAN WEIGHTS OF DETERMINATION FOR DIFFERENT EOS SENSOR COMBINATIONS: SMALLEST AND LARGEST MEDIAN ERROR, AND PERCENTAGE DEVIATION FROM MODIS-MISR SAMPLING

		MODIS-AM/ MISR 16–day	MISR 9–day	MODIS-AM 16–day	MISR 16–day	MODIS-AM/PM 16–day	MODIS-AM/ /PM/MISR 16–day
Models: All 3-Parameters Models							
Interpolation	Rnad	0.19–0.23	0.27–0.30	0.35–0.40	0.26–0.31	0.20–0.23	0.13–0.16
$\theta_s = \langle\theta_s\rangle$	bsa	0.16–0.18	0.21–0.25	0.32–0.55	0.21–0.21	0.18–0.29	0.11–0.14
Extrapolation	Rnad	0.45–1.35	0.61–2.00	1.17–6.61	0.58–1.49	0.67–3.50	0.36–1.11
$\theta_s = 0$	bsa	0.18–0.52	0.25–0.71	0.33–2.54	0.25–0.63	0.19–1.32	0.13–0.43
Global, $\int \theta_s d\theta_s$	wsa	0.34–0.42	0.42–0.56	0.99–1.60	0.34–0.42	0.55–0.95	0.27–0.38
Parameters	f_{vol}	0.15–1.86	0.22–2.45	0.39–7.23	0.16–1.84	0.23–4.20	0.12–1.65
	f_{geo}	0.27–0.86	0.37–1.22	0.68–4.56	0.28–0.88	0.39–2.43	0.22–0.77
Models: All 3-Parameter Models, with Ross-Thick/Li-Dense replaced by Ross-Thick and Li-Dense separately							
Interpolation	Rnad	0.18–0.23	0.25–0.30	0.30–0.40	0.23–0.31	0.17–0.23	0.12–0.16
$\theta_s = \langle\theta_s\rangle$	bsa	0.16–0.18	0.21–0.25	0.25–0.55	0.20–0.21	0.15–0.29	0.10–0.14
Extrapolation	Rnad	0.17–0.93	0.24–1.24	0.28–3.45	0.23–1.09	0.16–1.94	0.12–0.77
$\theta_s = 0$	bsa	0.18–0.28	0.25–0.37	0.29–0.82	0.24–0.36	0.17–0.45	0.12–0.23
Global, $\int \theta_s d\theta_s$	wsa	0.17–0.42	0.23–0.56	0.31–1.60	0.21–0.42	0.18–0.95	0.12–0.38
Parameters	f_{vol}	0.15–0.89	0.22–1.25	0.39–2.01	0.16–0.97	0.23–1.19	0.12–0.73
	f_{geo}	0.27–0.60	0.37–0.86	0.68–2.32	0.28–0.63	0.39–1.28	0.22–0.49
Models: All 3-Parameter Models, with Ross-Thick/Li-Dense replaced by Ross-Thick and Li-Dense separately							
Interpolation	Rnad	0, 0	+38, +30	+66, +73	+27, +34	−6, 0	−34, −31
$\theta_s = \langle\theta_s\rangle$	bsa	0, 0	+31, +38	+56, +205	+25, +16	−7, +61	−38, −23
Extrapolation	Rnad	0, 0	+41, +33	+64, +270	+35, +17	−6, +108	−30, −18
$\theta_s = 0$	bsa	0, 0	+38, +32	+61, +192	+33, +28	−6, +60	−34, −18
Global, $\int \theta_s d\theta_s$	wsa	0, 0	+35, +33	+82, +280	+23, 0	+5, +126	−30, −10
Parameters	f_{vol}	0, 0	+46, +40	+160, +125	+6, +8	+53, +33	−20, −18
	f_{geo}	0, 0	+37, +43	+151, +286	+3, +5	+44, +113	−19, −19

Rnad = reflectance at nadir view angle; bsa = black-sky albedo; wsa = white-sky albedo; f_{vol} = volume scattering kernel coefficient; f_{geo} = surface scattering kernel coefficient.

Table 3: RANGES OF WEIGHTS OF DETERMINATION FOR DIFFERENT EOS SENSOR COMBINATIONS: SMALLEST AND LARGEST ERROR IN THE WORST CASE, AND PERCENTAGE DEVIATION FROM MODIS-MISR SAMPLING

		MODIS–AM + MISR 16–day	MISR 9–day	MODIS–AM 16–day	MISR 16–day	MODIS–AM+PM 16–day	MODIS–AM +PM+MISR 16–day
Models: All 3-Parameter Models							
Interpolation	Rnad	0.18–0.28	0.25–0.36	0.29–0.54	0.25–0.38	0.17–0.28	0.12–0.18
$\theta_s = \langle\theta_s\rangle$	bsa	0.15–0.20	0.20–0.29	0.40–0.72	0.17–0.24	0.23–0.41	0.12–0.15
Extrapolation	Rnad	1.03–1.71	1.45–2.41	2.95–9.59	1.12–2.23	1.61–5.44	0.90–1.51
$\theta_s = 0$	bsa	0.39–0.63	0.53–0.94	0.80–4.01	0.51–0.76	0.45–1.95	0.29–0.61
Global, $\int \theta_s d\theta_s$	wsa	0.21–1.05	0.28–1.47	0.76–2.90	0.24–1.74	0.47–1.43	0.17–0.81
Parameters	f_{vol}	0.62–4.14	0.87–5.83	2.97–13.07	0.68–7.11	1.63–6.60	0.52–3.10
	f_{geo}	0.60–1.34	0.87–1.84	2.01–7.07	0.62–1.88	1.18–3.56	0.56–1.06
Models: All 3-Parameter Models, with Ross-Thick/Li-Dense replaced by Ross-Thick and Li-Dense separately							
Interpolation	Rnad	0.18–0.28	0.25–0.36	0.29–0.44	0.25–0.38	0.17–0.25	0.12–0.18
$\theta_s = \langle\theta_s\rangle$	bsa	0.15–0.20	0.20–0.29	0.40–0.72	0.17–0.24	0.23–0.41	0.12–0.15
Extrapolation	Rnad	0.73–1.08	0.96–1.58	1.47–5.72	0.77–1.54	0.86–3.18	0.60–1.05
$\theta_s = 0$	bsa	0.19–0.49	0.25–0.66	0.30–2.54	0.26–0.57	0.17–1.47	0.13–0.43
Global, $\int \theta_s d\theta_s$	wsa	0.21–0.82	0.28–1.11	0.66–2.42	0.24–0.92	0.40–1.41	0.17–0.67
Parameters	f_{vol}	0.33–1.76	0.48–2.48	1.21–3.52	0.37–3.28	0.72–1.97	0.28–1.08
	f_{geo}	0.45–0.69	0.62–0.95	0.99–3.73	0.47–0.98	0.58–1.99	0.40–0.59
Models: All 3-Parameter Models, with Ross-Thick/Li-Dense replaced by Ross-Thick and Li-Dense separately							
Interpolation	Rnad	0, 0	+38, +28	+61, +57	+38, +35	–6, –11	–34, –36
$\theta_s = \langle\theta_s\rangle$	bsa	0, 0	+33, +44	+166, +259	+13, +19	+53, +104	–20, –26
Extrapolation	Rnad	0, 0	+31, +46	+101, +429	+5, +42	+17, +194	–18, –3
$\theta_s = 0$	bsa	0, 0	+31, +34	+57, +418	+36, +16	–11, +200	–32, –13
Global, $\int \theta_s d\theta_s$	wsa	0, 0	+33, +35	+214, +195	+14, +12	+90, +71	–20, –19
Parameters	f_{vol}	0, 0	+45, +40	+266, +100	+12, +86	+118, +11	–16, –39
	f_{geo}	0, 0	+37, +37	+119, +440	+4, +42	+28, +188	–12, –15

Rnad = reflectance at nadir view angle; bsa = black-sky albedo; wsa = white-sky albedo; f_{vol} = volume scattering kernel coefficient; f_{geo} = surface scattering kernel coefficient.

Table 4: INFERRED EQUIVALENT WEIGHTS OF DETERMINATION FOR THE MODIFIED RPV MODEL: SMALLEST AND LARGEST MEDIAN ERROR, AND SMALLEST AND LARGEST ERROR IN THE WORST CASE

MODIS–AM/MISR 16-Day Sampling		Red Band median	Red Band worst-case range	NIR Band median	NIR Band worst-case range
Interpolation	Rnad	0.21–0.28	0.20–0.31	0.19–0.22	0.16–0.26
$\theta_s = \langle\theta_s\rangle$	bsa	0.08–0.16	0.14–0.18	0.04–0.06	0.05–0.09
Extrapolation	Rnad	0.32–0.49	0.38–0.76	0.31–0.49	0.38–0.76
$\theta_s = 0$	bsa	0.11–0.20	0.17–0.39	0.08–0.13	0.07–0.33
Global, $\int \theta_s d\theta_s$	wsa	0.19–0.23	0.16–0.49	0.17–0.19	0.10–0.36
Parameters	r_0	0.17–0.29	0.23–0.51	0.16–0.25	0.19–0.47
	k	1.70–9.86	4.37–15.25	0.89–1.41	0.98–2.00
	w_1	3.12–12.12	5.96–28.20	1.15–2.71	1.70–4.02
Land cover types (Kimes et al.): Corn, Lawn, Plowed Field, Hardwood Forest					

Rnad = reflectance at nadir view angle; bsa = black-sky albedo; wsa = white-sky albedo; r_0 = base reflectance coefficient; k = BRDF slope coefficient; w_1 = forward/backward scattering coefficient.

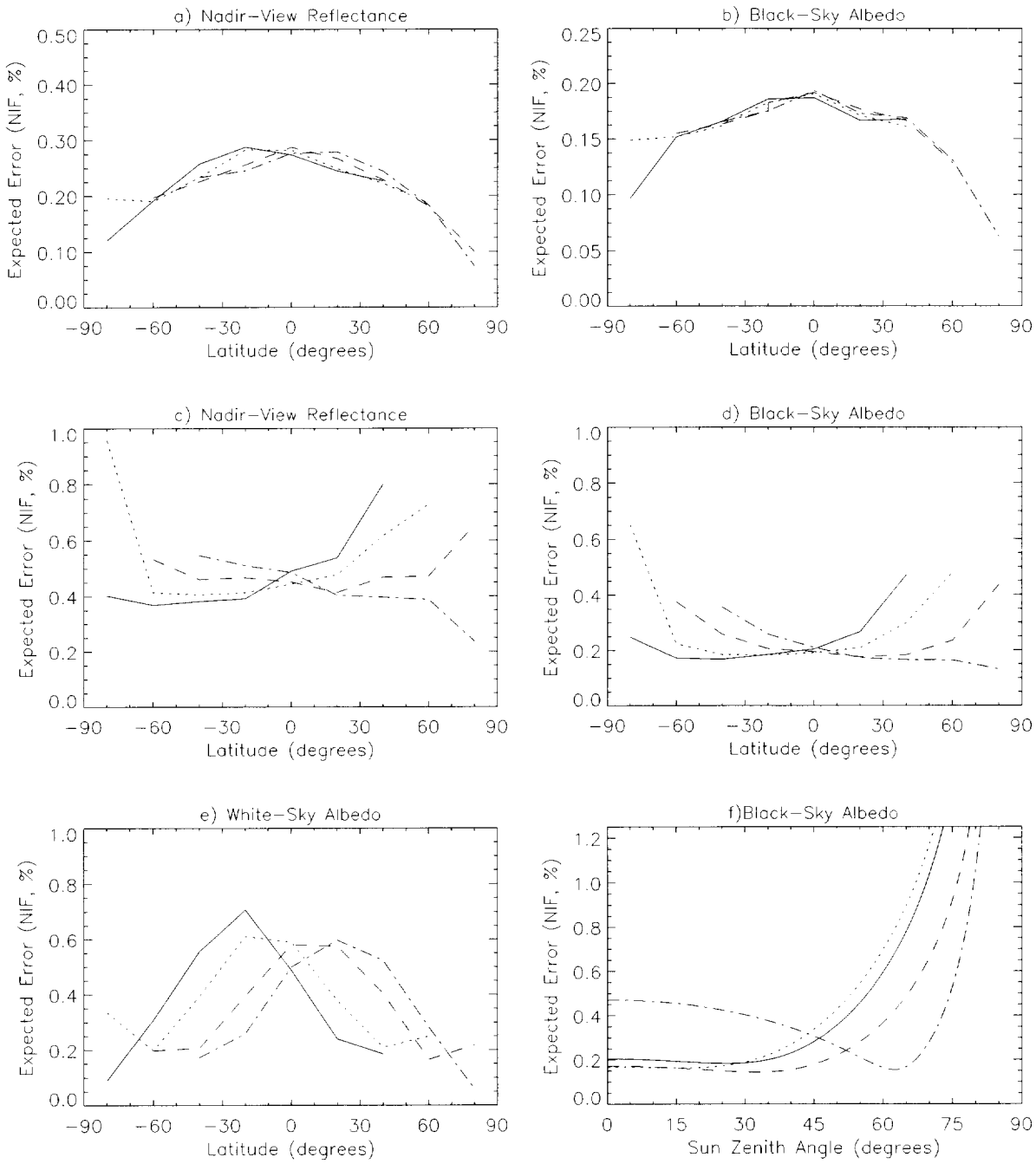

Figure 1: Noise sensitivity of the Ambrals BRDF model using the example of the RossThick-LiSparse kernel combination. Weights of determination ("Noise inflation factors", NIF) are shown as a function of latitude for different 16-day time periods throughout the first half of the year. Panel (f) shows the noise sensitivity of black-sky albedo extrapolation as a function of sun zenith angle for different latitudes and for sampling during the first 16-day period of the year.

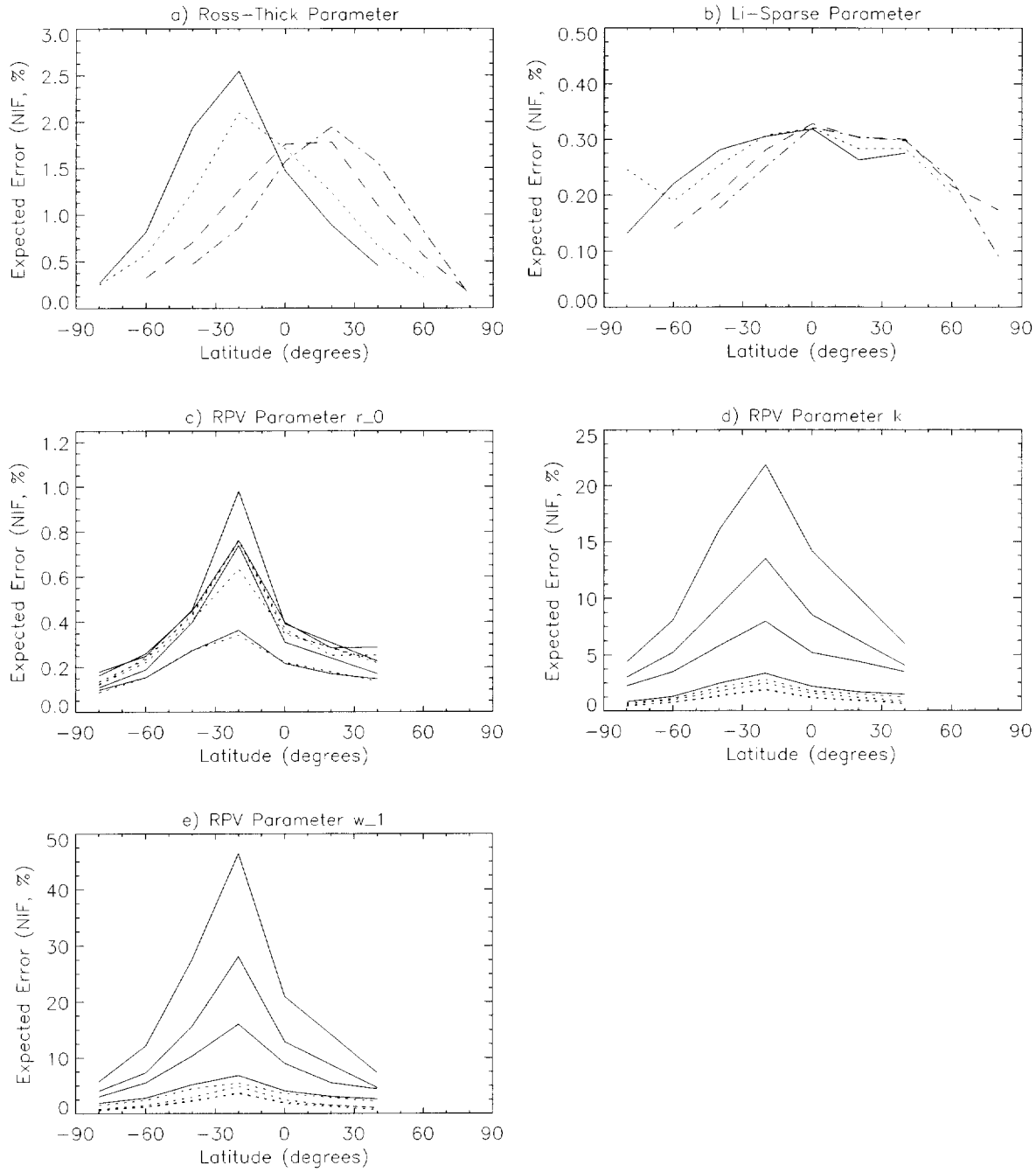

Figure 2: Noise sensitivity of the model parameters for the Ambrals BRDF model using the example of the RossThick-LiSparse kernel combination and the modified RPV BRDF model. Weights of determination ("Noise inflation factors", NIF) are shown as a function of latitude; for the Ambrals model they are shown for different 16-day time periods throughout the first half of the year, for the modified RPV model for sampling of the first of these 16-day periods and for the red and near-infrared band of four different land cover types (Ambrals model analysis is independent of band or land cover type due to the mathematical properties of kernel-driven models).

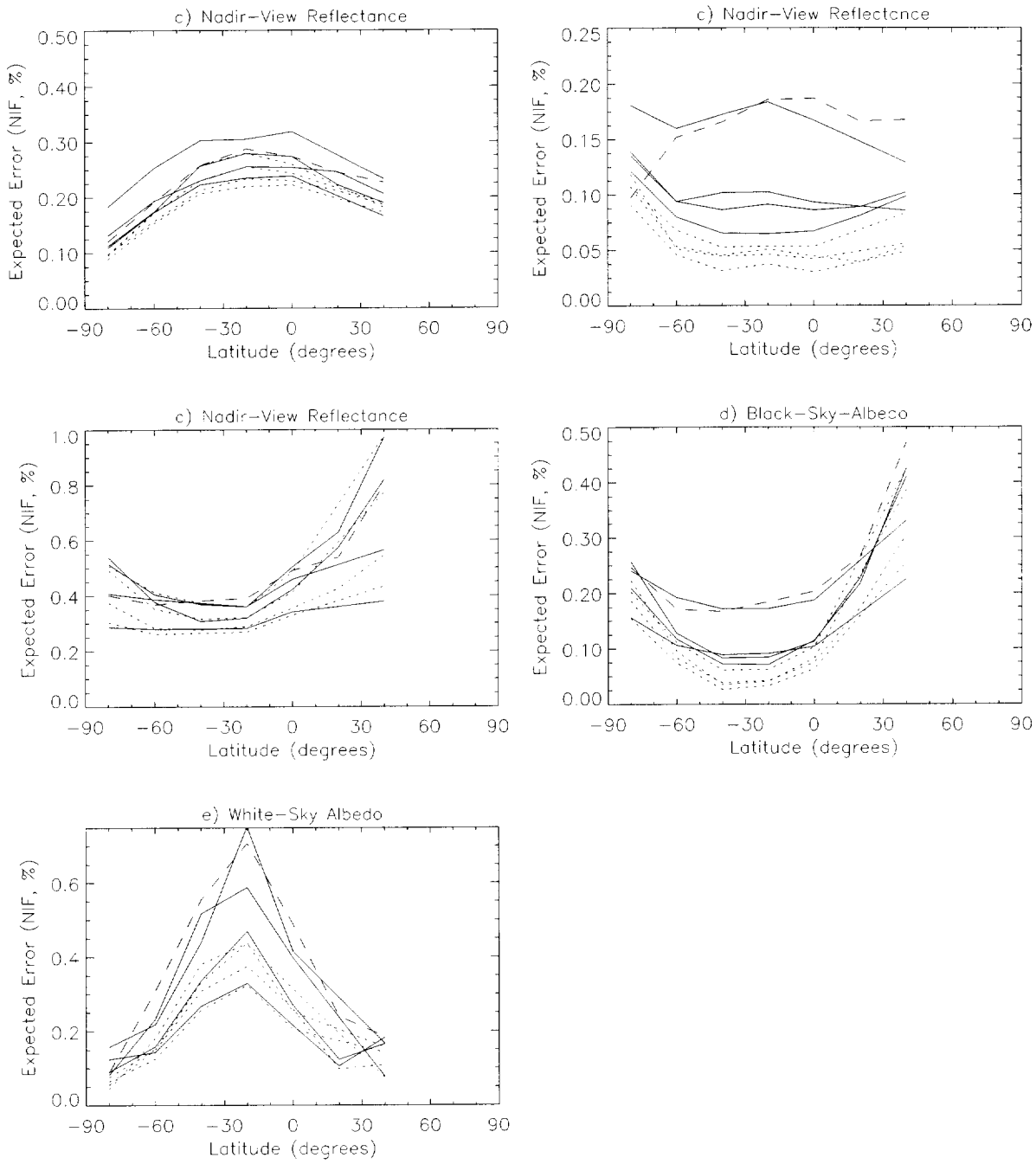

Figure 3: Noise sensitivity of the modified RPV BRDF model. Inferred equivalent weights of determination ("Noise inflation factors", NIF) are shown as a function of latitude for the first 16-day period of the year and for the red and near-infrared band of four different land cover types (solid and dotted lines). Also shown is are the weights of determination for the Ambrals BRDF models using the example of the RossThick-LiSparse kernel combination (dashed lines).